Adsorptive removal of gallic acid from aqueous solution onto magnetic ion exchange resin

Lei Ding, Changjin Guo, Yunhua Zhu, Jiangya Ma, Yanli Kong, Meiying Zhong, Qiongxi Cao and Huiwen Zhang

ABSTRACT

Finding an appropriate adsorbent with high adsorption capacity, quick adsorption kinetics and easy regeneration was crucial to the removal of gallic acid (GA) from water and wastewater. Our aims were to investigate whether a magnetic ion exchange (MIEX) resin had the three merits mentioned above, and investigate the feasibility of GA adsorption on MIEX resin, and the adsorption kinetics, equilibrium, thermodynamics, regeneration and mechanism using batch tests. The uptake of GA increased with increasing GA concentration. The GA concentration influenced the time needed to reach equilibrium, but the adsorption could be completed within 120 min. Elevating temperature facilitated the GA removal. The removal percent remained above 95.0% at pH 5.0–11.0. Carbonate and bicarbonate promoted the GA removal; conversely chloride, sulfate and nitrate restrained the GA removal significantly. The adsorption kinetics could be fitted well with the pseudo second-order model, and the film diffusion governed the whole adsorption rate. The equilibrium data followed the Redlich–Peterson isotherm model. The adsorption was a spontaneous, endothermic and entropy driven process. The ion exchange dominated the removal mechanism. The spent MIEX resin was well regenerated by sodium chloride. Therefore, MIEX resin is a potential adsorbent for removing GA quickly and efficiently from water and wastewater.

Key words | adsorption, equilibrium, gallic acid, ion exchange, kinetics, magnetic ion exchange resin

Lei Ding
Changjin Guo
Yunhua Zhu
Jiangya Ma
Yanli Kong
Meiying Zhong
Qiongxi Cao
Huiwen Zhang (corresponding author)
School of Civil Engineering and Architecture,
Anhui University of Technology,
59 Hudong Road, Maanshan 243002,
China
E-mail: *zhw@ahut.edu.cn*

Lei Ding
Jiangya Ma
Yanli Kong
Meiying Zhong
Huiwen Zhang
Engineering Research Center of Biomembrane Water Purification and Utilization Technology,
Ministry of Education,
Maanshan, Anhui, 243002,
China

INTRODUCTION

Gallic acid (3,4,5-trihydroxybenzoic acid, GA), as an important chemical, is widely used in many products including drugs, cosmetics and foods because of its antioxidant activity (Shahamirifard *et al.* 2018). A large amount of wastewater containing GA is discharged into the water environment during the production process of these products (Han *et al.* 2017). Related researches have demonstrated that GA in the water leads to the death of aquatic organisms and deteriorates water quality (Zhang *et al.* 2015). In addition, in the traditional drinking water treatment processes, such as coagulation, sedimentation, filtration and disinfection, it is difficult to remove the GA due to its water solubility and small molecular weight (Zhang *et al.* 2015). The unremoved GA causes an unpleasant color and odor in drinking water, and produces carcinogenic disinfection by-products during the chlorination process (Zhang *et al.* 2015; Celestino *et al.* 2018). Therefore, it is necessary to seek effective methods for reducing and removing GA from polluted raw water and wastewater.

Many technologies including electro-chemical oxidation, ozonation treatment, biological degradation, extraction and adsorption have been used to remove GA from water and wastewater (Rewatkar *et al.* 2016; Zhang *et al.* 2019). Among these methods, adsorption using different adsorbents has been extensively studied because of its convenient operation, high removal efficiency and adsorbent reusability (Celestino *et al.* 2018). Various adsorbents, such as clay minerals (Ahmat *et al.* 2019) and activated carbon (Chedri Mammar *et al.* 2019), have been utilized for the removal of GA. The small adsorption capacity of clay minerals limits its extensive application. Activated carbon has been used to remove GA, but regenerating spent activated carbon by thermal reactivation has some drawbacks such as high energy demand and loss of carbon

doi: 10.2166/wst.2020.236

(Chedri Mammar *et al.* 2019). Recently, various resins (Wang *et al.* 2009) have aroused more interest for the removal of GA due to their high adsorption capacity and easy regeneration compared with activated carbon, such as ZDX-1, WJN-09, XC-1, HP-2MG, XAD-7, XAD-761, XAD-4 and XAD-16. However, for these traditional resins, the large size (>0.4 mm) of resin particles leads to a slow kinetics. Therefore, finding an appropriate adsorbent with high adsorption capacity, quick adsorption kinetics and easy regeneration is helpful for the quick and efficient removal of GA from water and wastewater.

A new magnetic ion exchange (MIEX) resin, developed by Orica Watercare, is a macro-porous anion resin with two properties: smaller particle size (average 0.15 mm) and magnetism. MIEX resin has much more surface area because of being 2–5 times smaller than conventional resins. Consequently, MIEX resin may have potential for fast removing GA from water and wastewater due to its smaller size. In addition, in spite of having a small particle size, MIEX resin particles separate easily from water due to its magnetism. MIEX resin was mainly designed for the removal of dissolved organic matter from raw water and wastewater, and has been used to remove dissolved organic carbon, UV_{254}, geosmin, estrone, pesticides, etc (Boyer 2015; López-Ortiz *et al.* 2018). However, to our knowledge, the removal of GA by adsorption on MIEX resin has not been reported yet. So, investigating the feasibility of GA adsorption on MIEX resin and adsorption kinetics, equilibrium, thermodynamics, regeneration and mechanism will provide theoretical support for the application of MIEX resin and the design of an adsorption reactor.

Accordingly, the purpose of this study is to systematically evaluate the removal characteristics of GA by MIEX resin. In this work, the kinetics, equilibrium, and thermodynamics processes of GA adsorption on MIEX resin were determined. And the effects of solution pH and coexisting anions were investigated. The regeneration and circular utilization of MIEX resin were evaluated. MIEX resin is an excellent candidate for the removal of GA from water and wastewater.

MATERIALS AND METHODS

Materials and chemicals

MIEX resin, used as adsorbent in this study, was virgin resin supplied by Beijing Sino-Australia Orica Watercare Technology & Equipment Co., Ltd. GA was used as adsorbate. A standard stock solution (1,000 mg L^{-1}) of GA was prepared by dissolving 0.5051 g of GA (99% purity) in 0.5 L of ultrapure water. The working solution of desired GA concentrations was obtained by diluting the standard stock solution. Sodium carbonate (Na_2CO_3), sodium bicarbonate ($NaHCO_3$), sodium sulfate (Na_2SO_4), sodium chloride (NaCl) and sodium nitrate ($NaNO_3$) were used to simulate carbonate (CO_3^{2-}), bicarbonate (HCO_3^-), sulfate (SO_4^{2-}), chloride (Cl^-) and nitrate (NO_3^-) in water, respectively. The pH of solution was adjusted by 0.01 mol L^{-1} sodium hydroxide (NaOH) or hydrogen chloride (HCl). All chemicals used in this study were guaranteed analytical reagent or above grade and were purchased from Sinopharm Chemical Reagent Co., Ltd, China.

Analytical methods and instruments

Gallic acid was analyzed using an ultraviolet spectrophotometer (UV9600, Ruili, Beijing, China) at 264 nm (Celestino *et al.* 2018). The chloride ion was detected using an ion chromatograph (IC-2010 PLUS, Shimadzu, Japan). And the pH of solution was measured using a pH meter (pHS-3C model, Leici, China). All samples were carried out in triplicate and the average values are reported.

Adsorption experiments

Many parameters including adsorbent, adsorbate and environmental factors affect the removal of the GA. The pre-experiments showed that the MIEX resin particles and aqueous solution were mixed well and the effect of agitation speed could be neglected when the speed exceeded 150 rpm. Accordingly, the agitation speed was set at 150 rpm in this study. In addition, the adsorbent dosage was not selected as a parameter in this study because adsorbent dosage depends on the capacity of adsorbent and we conducted the adsorption equilibrium tests and obtained the equilibrium capacity of MIEX resin.

In order to better understand the adsorption kinetics, equilibrium, thermodynamics and mechanism of GA on MIEX resin, batch adsorption tests were performed at different parameters including contact time (0–180 min), initial GA concentration (5–20 mg L^{-1}), initial pH of solution (3–11), coexistent anions (1 meq L^{-1}) and temperatures (293–313 K). In a typical test, 0.5 mL of MIEX resin was added into a set of 500 mL solutions containing a certain concentration of GA. These slurries were agitated at a certain temperature with a stirring speed of 150 rpm for a period of time in a jar test apparatus (MY3000-6B, Qianjiang Meiyu Instrument Co., Ltd). After adsorption, the supernatant was

filtered using a 0.45 μm micro-filtration membrane, and the concentration of GA in the filtrate was determined using the UV9600 at a wavelength of 264 nm.

The amount of GA adsorbed onto MIEX resin at time t and the removal percent (E) of GA are calculated according to the Equations (1) and (2), respectively.

$$q_t = (C_0 - C_t)V/W \quad (1)$$

$$E = (C_0 - C_t)/C_0 \times 100\% \quad (2)$$

where q_t (mg mL^{-1}) is the amount of GA at time t (minutes); C_0 and C_t (mg L^{-1}) are the GA concentration at the initial and time t, respectively; V (L) is the volume of solution; W (mL) represents the MIEX resin volume.

When adsorption reaches equilibrium, Equation (1) can be expressed by Equation (3):

$$q_e = (C_0 - C_e)V/W \quad (3)$$

where q_e (mg mL^{-1}) is the amount of GA adsorbed at equilibrium; C_e (mg L^{-1}) is the GA concentration in solution at equilibrium.

Regeneration and reusability

The reusability of MIEX resin saturated with GA was investigated by regeneration. Half a milliliter of MIEX resin was regenerated by 500 mL of NaCl solution with the concentration of 0.5%. The regeneration tests were conducted in a jar test apparatus (MY3000-6B) at 150 rpm for 120 min. After desorption, the resin was separated through a 0.45 μm micro-filtration membrane and washed by an excess amount of ultrapure water. Afterwards, the regenerated resin was used as the adsorbent to adsorb GA to evaluate the regeneration efficacy. High removal efficacy of GA represents good regeneration. The recyclability of MIEX resin was studied by successive adsorption–desorption cycles.

RESULTS AND DISCUSSION

Adsorption kinetics

Effect of adsorption time and initial GA concentration

The time required to reach adsorption equilibrium determines the size of adsorption reactor. Figure 1 presents the effect of adsorption time on the GA removal at different initial GA concentrations (5, 10, 15 and 20 mg L^{-1}). It can be observed in Figure 1 that the trend of GA removal on MIEX resin is similar at different initial GA concentrations. At the initial stage, the amount of GA adsorbed on MIEX resin increases dramatically. This may be attributed to the fact that the resin is virgin and the active adsorption sites

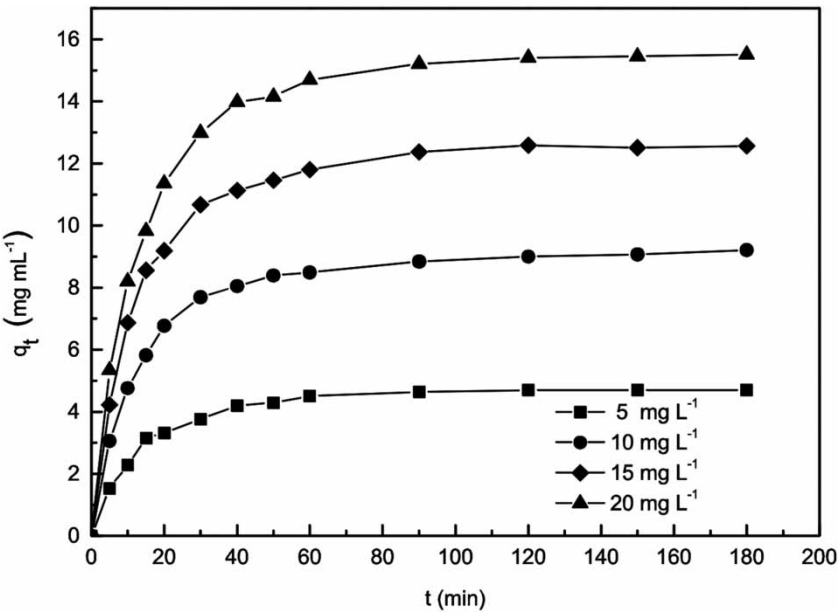

Figure 1 | Effects of initial GA concentration and adsorption time on the removal of GA on MIEX resin.

available are relatively sufficient in the initial stage, leading to the swift increase in uptake of GA (Ding *et al.* 2017). As the adsorption proceeds, the availability of active sites is gradually reduced. This makes it difficult for GA to be adsorbed on the resin, leading to the decrease in the adsorption rate (Akram *et al.* 2017). Finally, the adsorption gradually reaches equilibrium. Many researchers also found the same phenomenon that GA was adsorbed rapidly on adsorbents in the initial stage, and then the equilibrium was reached slowly (Wang *et al.* 2009).

On the other hand, Figure 1 demonstrates that the different initial GA concentrations have a slight effect on the required time to reach equilibrium. At the low GA concentration (5 and 10 mg L^{-1}), it takes approximately 60 min to attain equilibrium. However, reaching equilibrium needs 90–120 min at the high GA concentration (15 and 20 mg L^{-1}). The active sites of MIEX resin include internal sites as well as the external sites. When the GA concentration is low, the external sites are relatively sufficient and occupied firstly by GA molecules (Zhu *et al.* 2015). The external adsorption is relatively fast, which may be the reason why it takes relatively short time to reach equilibrium at low GA concentration (Yu *et al.* 2018). Yet at high GA concentration, besides external adsorption, GA molecules may be driven into the internal pores of MIEX resin by the greater concentration gradient (Li *et al.* 2013). The diffusion of GA molecules in the internal pores is much lower than the external adsorption (Perez-Aguilar *et al.* 2011). This may be the reason for the longer time needed to reach equilibrium at high GA concentration. Meanwhile, the amount of GA adsorbed on MIEX resin at high GA concentration is much larger because of full utilization of internal active sites of resin (Abdi *et al.* 2017). For the conventional resins used for the GA removal, attaining equilibrium usually needs more than 6 h due to the larger particle size (Wang *et al.* 2009). Therefore, MIEX demonstrates an obvious advantage in the much shorter adsorption time for the GA removal compared with the conventional resins.

Kinetic model of GA adsorbed on MIEX resin

Many models have been developed to predict the uptake rate of the adsorbate onto the adsorbent. Considering the fact that the pseudo first-order model and pseudo second-order model are the two most commonly used empirical models in liquid adsorption studies for batch processes (Tan & Hameed 2017), the two models are chosen to fit the kinetic data in this study. In addition, the Elovich model is also used because of well describing chemisorption. The three models can be expressed as Equations (4)–(6) (Tan & Hameed 2017), respectively.

Pseudo first-order model:

$$q_t = q_e(1 + e^{-k_1 t}) \tag{4}$$

Pseudo second-order model:

$$q_t = k_2 q_e^2 t/(1 + k_2 q_e t\,) \tag{5}$$

Elovich model:

$$q_t = \frac{1}{\beta}\ln(1 + \alpha\beta t) \tag{6}$$

where q_e and q_t represent the amount of GA adsorbed on MIEX resin (mg mL^{-1}) at equilibrium and any time t, respectively; k_1 (min^{-1}) and k_2 (mL mg^{-1} min^{-1}) are the kinetic constants for the pseudo first-order and the pseudo second-order, respectively; α is the initial adsorption rate (mg mL^{-1} min^{-1}); and β is the adsorption constant (mL mg^{-1}).

The fitted results are shown in Table 1. The correlation coefficient (R^2) and standard error (SE) are used to quantitatively compare the applicability of different kinetic models. A higher R^2 and lower SE represent a better fitting. According to Table 1, the pseudo second-order model can better fit the sorption of GA onto MIEX resin with the higher correlation coefficients ($R^2 > 0.99$) and lower standard errors (SE = 0.1248–0.3197) than those of the pseudo first-order and Elovich models. Accordingly, the pseudo second-order model is the most suitable to express the kinetic process of GA adsorption on MIEX resin. The pseudo second-order model is assumed to fit chemical reaction controlled kinetics (Riahi *et al.* 2017). This indicates that the adsorption of GA adsorbed on MIEX resin may involve chemisorption. Many studies found the pseudo second-order model could well model most environmental kinetic adsorption, asserting its superiority to other models (Tan & Hameed 2017). But some theoretical interpretations revealed that successful fitting of the pseudo second-order model alone was no guarantee of chemisorption control, and diffusion or combined diffusion–reaction control was also possible (Senthil Kumar *et al.* 2010).

Diffusion mechanism of GA

Previous research has demonstrated that the adsorption rate is generally controlled by three factors (Yoro *et al.* 2020): film diffusion, intra-particle diffusion and actual adsorption. In general, the adsorption rate of the actual adsorption is

Table 1 | The results fitted by pseudo first-order, pseudo second-order and Elovich models

Pseudo first-order model

C_0 (mg L^{-1})	$q_{e,exp}$ (mg mL^{-1})	$q_{e,cal}$ (mg mL^{-1})	k_1 (min^{-1})	R^2	SE
5	4.70	4.60	0.0068	0.98	0.1476
10	9.21	8.84	0.0729	0.98	0.2479
15	12.57	12.20	0.0763	0.98	0.3849
20	15.51	15.11	0.0724	0.98	0.4212

Pseudo second-order model

C_0 (mg L^{-1})	$q_{e,exp}$ (mg mL^{-1})	$q_{e,cal}$ (mg mL^{-1})	k_2 (mL mg^{-1} min^{-1})	R^2	SE
5	4.70	5.14	0.0180	0.99	0.1248
10	9.21	9.86	0.0102	0.99	0.1817
15	12.57	13.56	0.0078	0.99	0.2515
20	15.51	16.81	0.0060	0.99	0.3197

Elovich model

C_0 (mg L^{-1})	α (mg mL^{-1} min^{-1})	β (mL mg^{-1})	R^2	SE
5	0.5184	0.89	0.91	0.3197
10	1.2844	1.67	0.91	0.5938
15	2.0398	2.25	0.90	0.8307
20	2.2555	2.83	0.91	1.0232

accepted to be very fast and the effect on the rate of adsorption can be negligible, and the overall rate of adsorption can be controlled by the film diffusion or/and intra-particle diffusion (Sun *et al.* 2011).

Many diffusion models have been developed to describe the diffusion process, such as Boyd model, linear film diffusion model, Weber–Morris model, Vermeulen model, and Bangham model (Tan & Hameed 2017). Among these models, Boyd model and linear film diffusion model are mainly used to describe the liquid film diffusion process. However, Weber–Morris model, Vermeulen model, and Bangham model can be used to check whether the intra-particle diffusion is the sole rate-controlling mechanism. In this study, we adopt the Weber–Morris model and Boyd model to further identify the diffusion mechanism of the adsorption of gallic acid onto MIEX resin, because of their simple equations.

The Weber–Morris model and Boyd model can be expressed in Equations (7) and (8) (Tan & Hameed 2017).

$$q_t = k_{id} t^{1/2} + C_i \tag{7}$$

$$Bt = -0.4977 - \ln(1 - q_t/q_e) \tag{8}$$

where k_{id} is the intra-particle diffusion rate constant (mg mL^{-1} min$^{-1/2}$); C_i is the model constant associated with the thickness of the boundary layer; B is a constant.

For Weber–Morris model, the results of q_t versus $t^{1/2}$ at different initial GA concentrations are presented in Figure 2(a). The linear regression parameters (k_{id}, C_i) and correlation coefficients (R^2) are presented in Table 2. According to the intra-particle diffusion theory, if the adsorption process is only controlled by the intra-particle diffusion, the plot of q_t against $t^{1/2}$ should be a straight line and pass through the origin (Kim & Choi 2017). Figure 2(a) shows that plots of q_t vs. $t^{1/2}$ are not linear throughout the adsorption time, but each plot is divided into three segments that have a good linear form. However, each segment does not pass through the origin. This implies that the intra-particle diffusion is not the only rate-limiting step for the whole reaction (Wang *et al.* 2009). Also, Table 2 shows that the values of C_i ($i = 1$, 2 or 3) are not equal to 0. This further indicates that more than one diffusion process affects the adsorption. In fact, in most studies, this plot shows multilinearity over the entire adsorption period. Multilinearity may be an indication of multiple mechanisms that control the process, and each

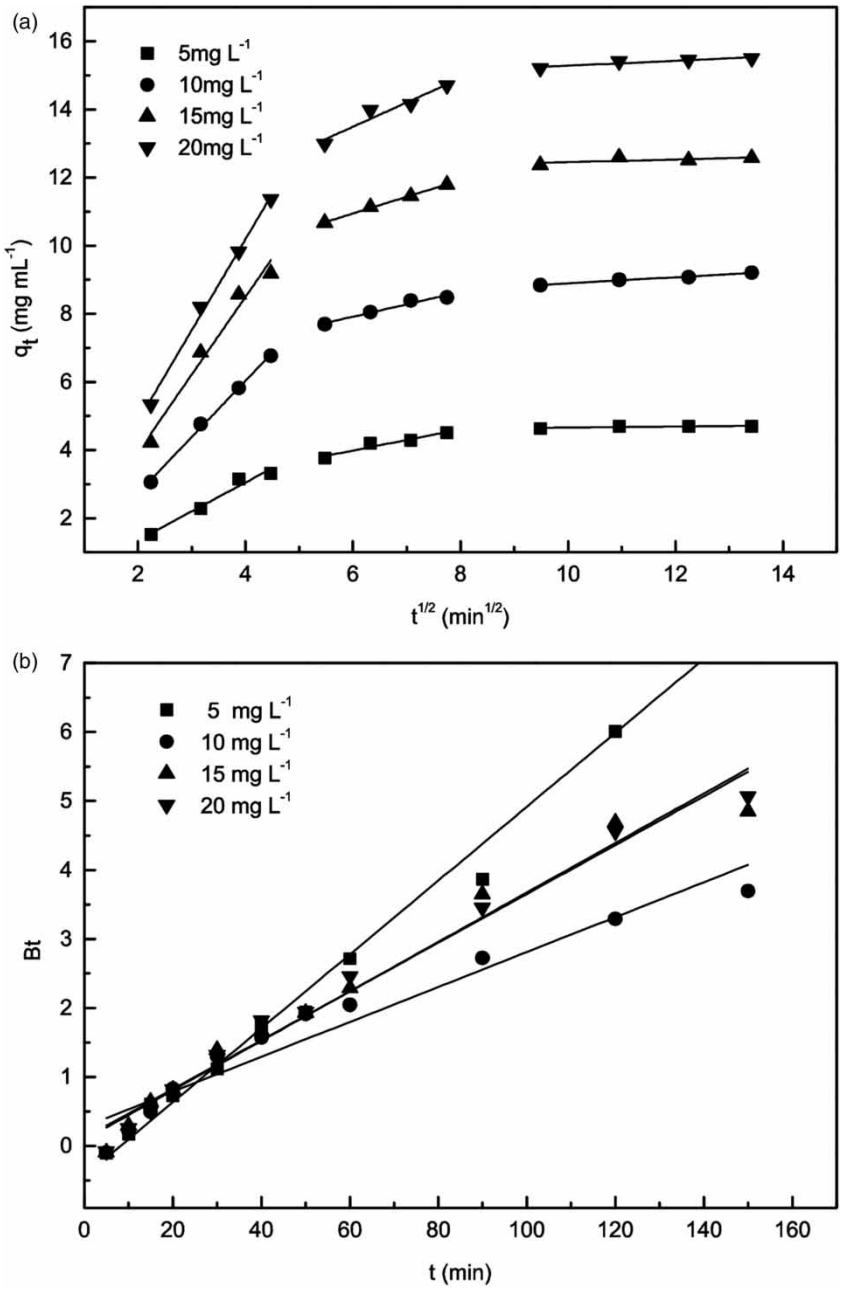

Figure 2 | (a) Intra-particle and (b) Boyd film diffusion kinetics for adsorption of GA by MIEX resin.

Table 2 | Constants and correlation coefficients of intra-particle diffusion model for GA adsorbed on MIEX resin

	Intra-particle diffusion model								
C_0 (mg L^{-1})	k_{id1} (mg mL^{-1} $min^{-1/2}$)	C_1	R^2	k_{id2} (mg mL^{-1} $min^{-1/2}$)	C_2	R^2	k_{id3} (mg mL^{-1} $min^{-1/2}$)	C_3	R^2
5	0.846	−0.34	0.95	0.310	2.13	0.91	0.014	4.52	0.47
10	1.650	−0.57	0.99	0.363	5.74	0.95	0.090	8.00	0.97
15	2.278	−0.62	0.96	0.491	8.00	0.99	0.041	12.04	0.24
20	2.671	−0.49	0.99	0.711	9.23	0.91	0.072	14.56	0.85

linear segment represents a controlling mechanism or several simultaneous controlling mechanisms (Tan & Hameed 2017). In the initial step, external surface adsorption or instantaneous adsorption occurs. In the second step, the intraparticle diffusion begins. In the third step, the system approaches equilibrium. Adsorption slows as surface coverage nears saturation.

In order to further determine the actual rate-controlling step involved in the adsorption process, the Boyd model is used to fit the kinetic data of GA adsorbed on MIEX resin, and results are shown in Figure 2(b) and Table 3.

It can be seen from Figure 2(b) that the plots of *Bt* versus *t* have a good linear form within the whole adsorption time at different initial GA concentrations, but they do not pass through the origin. This indicates that the adsorption process of GA on MIEX resin may be governed by the film diffusion (Yoro *et al.* 2020). In addition, the values of *B* (0.0253–0.0536) at different initial GA concentrations are far less than 1 and the linear correlation coefficients are high ($R^2 > 0.94$), further verifying the fact that the adsorption of GA on MIEX resin is governed by the film diffusion (Viegas *et al.* 2014).

Table 3 | The results of Boyd model at different initial concentrations

C_0 (mg L^{-1})	*B*	R^2
5	0.0536	0.99
10	0.0253	0.94
15	0.0354	0.97
20	0.0359	0.98

Equilibrium of GA adsorbed on MIEX resin

Adsorption equilibrium

The temperature of the solution is one of the key roles in the solid–liquid adsorption system. The adsorption equilibrium of GA on MIEX resin at 293, 303, and 313 K is shown in Figure 3. Figure 3 shows the adsorptivity of GA increases with the increase in temperature, demonstrating that the adsorption process of GA on MIEX resin is an endothermic reaction. Elevating temperature favors the removal of GA (Hamayun *et al.* 2014). The higher temperature decreases the viscosity of the solution, causing the increase in the mobility of the GA ions and the decrease in the retarding forces acting on the diffusing ions (Li *et al.* 2010). Therefore, it is easy for the activated GA ions to enter into the internal pore to make full use of the internal active sites (Singh & Kushwaha 2014). This may be the reason that elevating temperature increases the adsorption capacity of GA. Similar

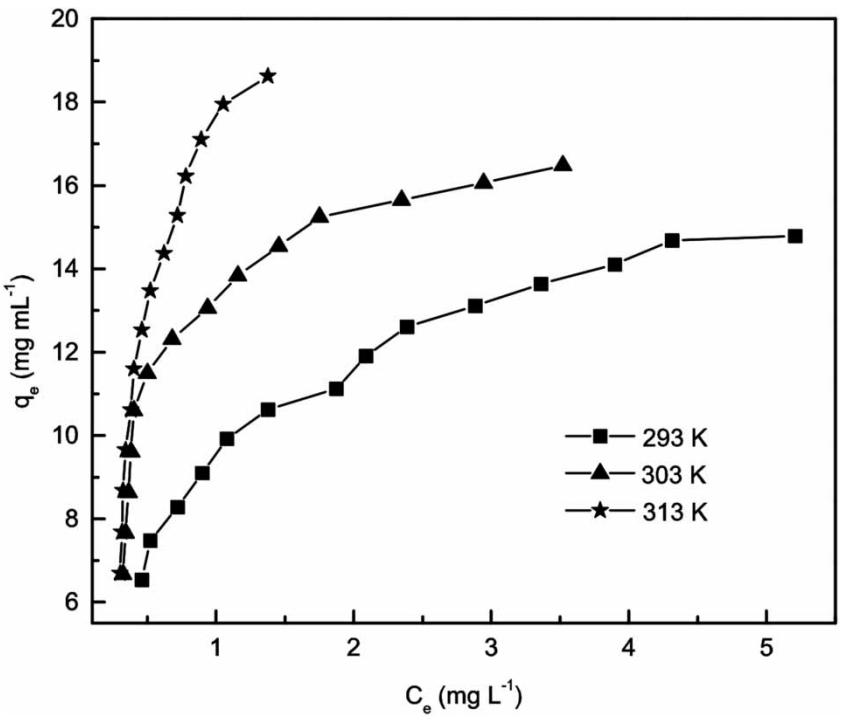

Figure 3 | The results of adsorption equilibrium of GA adsorbed on MIEX resin at different temperatures.

phenomena were found for other adsorbents, such as P115 (Ignat *et al.* 2011) and AB-8 resin (Gao *et al.* 2013).

Isotherm model of GA adsorbed on MIEX resin

The correlation of equilibrium adsorption data by theoretical or empirical equations is important in the design and operation of adsorption systems. Many equilibrium models have been developed to describe the adsorption equilibrium, such as Langmuir model, Freundlich model, Temkin model, Dubinin–Radushkevich model, and Redlich–Peterson model (Foo & Hameed 2010). We adopt the most widely used two-parameter isotherm models, Langmuir model and Freundlich model, to fit the equilibrium data. As a three-parameter model, Redlich–Peterson model is also used in this study. And the expressions of these models are given by Equations (9)–(11) as follows (Foo & Hameed 2010).

Langmuir isotherm model:

$$q_e = q_{\max} K_L C_e / (1 + K_L C_e) \tag{9}$$

Freundlich isotherm model:

$$q_e = K_F C_e^{\frac{1}{n}} \tag{10}$$

Redlich–Peterson isotherm model:

$$q_e = K_{RP} C_e / (1 + A_{RP} C_e^{B_{RP}}) \tag{11}$$

where $q_{\max}$ (mg mL^{-1}) is the theoretical maximum GA uptake, and K_L (L mg^{-1}) is the Langmuir isotherm model constant; K_F (mg mL^{-1}(L mg^{-1})$^{1/n}$) represents the Freundlich isotherm model constant and $1/n$ is the heterogeneity factor of the adsorbent; K_{RP}, A_{RP} and B_{RP} are the Redlich–Peterson isotherm model constants.

The essential features of the Langmuir isotherm dimensionless separation factor (R_L) are given by the Equation (12) (Doke & Khan 2017):

$$R_L = 1/(1 + K_L C_0) \tag{12}$$

The fitted results of these isotherms are separately presented in Table 4. Compared with the Freundlich model, the fitting to equilibrium data with the Langmuir model is better with higher values of correlation coefficient ($R^2 >$ 0.94) and lower values of standard error (SE = 0.3559–0.9838), which indicates that the adsorption process is mainly monolayer adsorption (Doke & Khan 2017).

Table 4 | The results of isotherm models for GA adsorbed on MIEX resin

Langmuir model

T (K)	q_{max} (mg mL^{-1})	K_L (L mg^{-1})	R_L	R^2	SE
293	16.61	1.3573	0.0355–0.0952	0.98	0.3559
303	18.43	2.5926	0.0189–0.0522	0.94	0.7801
313	30.75	1.3259	0.0363–0.0923	0.94	0.9838

Freundlich model

T (K)	K_F	$1/n$	R^2	SE
293	9.3102	0.3083	0.98	0.3852
303	12.4436	0.2747	0.87	1.1913
313	17.3823	0.5344	0.89	1.2935

Redlich–Peterson model

T (K)	K_{RP}	A_{RP}	B_{RP}	R^2	SE
293	36.8637	2.8989	0.8495	0.99	0.2342
303	39.2912	1.8899	1.1007	0.94	0.7749
313	29.1231	0.6310	1.9445	0.96	0.7468

Meanwhile, the value of separation factor R_L (0.0189–0.0952) indicates the adsorption isotherm to be favorable (Doke & Khan 2017). But the Redlich–Peterson isotherm model gives the best fittings with highest correlation coefficients (R^2: 0.94–0.99) and lowest values of standard error (SE: 0.2342–0.7749). This may be attributed to the fact that the Redlich–Peterson model combines the characteristics of Langmuir and Freundlich models, resulting in a wider range of applications (Prasad & Srivastava 2009).

Adsorption thermodynamics

Thermodynamic parameters of GA adsorbed on MIEX resin

Thermodynamic analysis can provide information to better understand the inherent energy change and mechanism involved in the adsorption process. The thermodynamics parameters of standard enthalpy change (ΔH^0, kJ mol^{-1}), standard entropy change (ΔS^0, J K^{-1} moL^{-1}) and standard Gibbs free energy change (ΔG^0, kJ moL^{-1}), are calculated using the following Equations (13)–(15):

$$K_D = (C_0 - C_e)V / C_e W \tag{13}$$

$$\ln K_D = \Delta S^0 / R - \Delta H^0 / RT \tag{14}$$

$$\Delta G^0 = \Delta H^\circ - T\Delta S^\circ \tag{15}$$

where K_D (L mL^{-1}) is the distribution coefficient, R (8.314 J mol^{-1} K^{-1}) is the universal gas constant and T is the absolute temperature (K).

Thermodynamic parameters for GA adsorbed on MIEX resin at different temperature are given in Table 5. The negative values of ΔG^0 at all investigated temperatures indicate that the adsorption of GA onto MIEX resin is a spontaneous process. Meanwhile, the values of ΔG^0 become more negative with increasing temperature, confirming that adsorption is more favorable at higher temperature. The calculated ΔH^0 values are positive, demonstrating the endothermic nature of GA adsorbed on MIEX resin. The above conclusions are consistent with the results in the adsorption equilibrium study. In addition, the positive ΔS^0 values reveal the good affinity of GA adsorbed on MIEX resin. Therefore, the adsorption is a spontaneous, endothermic and entropy driven process.

Activation energy of GA adsorbed on MIEX resin

In a solid–liquid adsorption process, the activation energy (E_a, KJ moL^{-1}) of the reaction refers to the minimum energy required for the molecule to participate in the reaction, and its value can be used to determine the type of adsorption. It is calculated using the following Arrhenius Equation (16):

$$\ln k = \ln A - E_a/RT \tag{16}$$

Table 5 | Thermodynamic parameters of GA adsorbed on MIEX resin

C_0 (mg L^{-1})	ΔH^0 (kJ mol^{-1})	ΔS^0 (J K^{-1} moL^{-1})	ΔG^0 (kJ moL^{-1})		
			293 K	303 K	313 K
7	16.63	79.18	−6.57	−7.36	−8.15
8	20.03	90.90	−6.60	−7.51	−8.42
9	32.12	130.67	−6.16	−7.47	−8.78
10	38.92	15,303	−5.91	−7.44	−8.97
11	41.57	161.60	−5.78	−7.39	−9.01
12	57.44	211.67	−4.58	−6.70	−8.81
13	57.06	209.43	−4.30	−6.39	−8.49
14	57.06	209.43	−4.30	−6.39	−8.49
15	55.93	204.75	−4.06	−6.11	−8.16
16	58.20	211.06	−3.64	−5.75	−7.87
17	61.60	221.54	−3.31	−5.53	−7.74
18	62.73	224.03	−2.91	−5.15	−7.39
19	60.84	216.77	−2.67	−4.84	−7.01
20	59.33	210.18	−2.25	−4.35	−6.45

where k is the rate constant at different temperatures obtained from the pseudo second-order kinetic model; A is the Arrhenius factor, R is the gas constant (8.314×10^{-3} KJ moL^{-1} K), and T (K) is the absolute temperature.

The adsorption kinetics of GA adsorbed on MIEX is obtained at 293, 303 and 313 K. The pseudo second-order kinetic model is used to fit the above kinetic data, and the values of k at 293, 303 and 313 K are 0.0036, 0.0038 and 0.0044, respectively. The linear plot of ln k against $1/T$ is presented in Figure 4. The value of E_a calculated from the slope of the linear plot is 8.499 KJ moL^{-1}, indicating that the adsorption process is a chemical adsorption (El-Shahawi & Nassif 2003). Meanwhile, the positive value of E_a also demonstrates the endothermic nature of the adsorption process.

Effect of initial pH of solution

Solution pH is considered to be an important parameter because it affects not only the surface properties of adsorbent but also the ionization of adsorbate (Gil *et al.* 2019). The effects of initial pH of solution on the removal of GA on MIEX resin are shown in Figure 5(a). As is clearly shown in Figure 5(a) the removal percent of GA dramatically increases from 11.31% to 93.59% with increasing pH from 3.0 to 5.0, and remains approximately constant above 96.0% when pH > 6.0. This may be interpreted by the different dissociation degrees of GA at different pHs (Celestino *et al.* 2018). The theoretical distribution curves of GA species at different pHs (Figure 5(b)) can verify the above assumption (Fazary & Ju 2008; Celestino *et al.* 2018). GA dissociates by about 10% at pH 3.0 (shown in Figure 5(b)), and the removal efficiency of GA is 11.31% accordingly at this pH. At pH 6.0, 95% of GA is ionized, and the removal of GA is 96.37%. As an anion exchange resin, the higher the ionization of GA, the higher the removal percent of GA due to ion exchange reaction. The corresponding relationship between the degree of ionization of GA and its removal efficiency at different pHs suggests that ion exchange dominates the removal mechanism of GA on MIEX resin. Regarding the effect of pH, some studies using other adsorbents for the removal of GA reported similar results (Celestino *et al.* 2018; Ahmat *et al.* 2019). However, compared with using MIEX resin for the removal of anions (such as bromide, bromate, chlorite), the optimal pH ranged from 5.0 to 8.0, and the removal of anions decreased significantly due to the competition of hydroxyl ions (Ding *et al.* 2012; Tang *et al.* 2013; Zhu *et al.* 2015). Therefore, MIEX

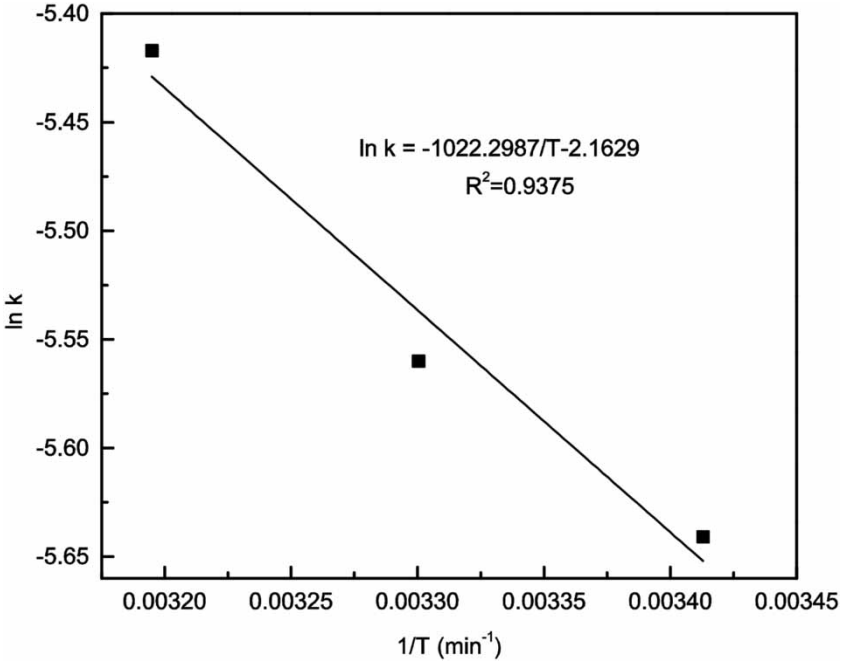

Figure 4 | The plot of calculating the activation energy for the GA adsorbed on MIEX resin.

resin has a great advantage for the removal of GA at a wide range of pH.

Effect of coexistent anions

It is well known that some inorganic anions such as CO_3^{2-}, HCO_3^-, SO_4^{2-}, Cl^- and NO_3^- are present in natural waters. Therefore, this experiment explores the effects of several common anions in water on the removal of GA by adsorption on MIEX resin and the results are given in Figure 6. Compared with the absence of inorganic anions, the removal efficiency slightly increases with the presence of CO_3^{2-} or HCO_3^- in solution. The slight promotion may be attributed to the fact that the hydroxyl groups on the phenyl ring of GA gradually dissociate in the alkaline environment caused by CO_3^{2-} or HCO_3^-, and the ionized GA molecules are easy to be removed by ion exchange with the chloride ions on the surface of MIEX resin. Also, we found the same phenomenon in our research on the removal of phosphate on MIEX resin (Ding *et al.* 2012). Conversely, SO_4^{2-}, Cl^- or NO_3^- competes with GA for the active sites on the surface of MIEX resin, causing a decrease in the removal of GA (Boyer 2015). A similar negative influence was reported using MIEX resin for the removal of other organics and anions (Boyer 2015; Zhu *et al.* 2015). Generally speaking, the affinity of different ions to the active sites of resin obeys the rule as follows: trivalent anion > divalent anion > monovalent anion (Ding *et al.* 2012). This can be used to interpret the fact (demonstrated in Figure 6) that the adverse effect of sulfate ions on the removal of GA is much stronger than that of chloride and nitrate.

Regeneration of spent MIEX resin

The adsorption–desorption process of GA on MIEX resin is repeated for 10 times, and the results are shown in Figure 7. As can be seen in Figure 7, the removal percent of GA by regenerated MIEX resin gradually decreases with the increase in the number of adsorption–desorption cycles, but the MIEX resin can maintain relatively high GA removal efficiency (73.54%) even after 10 cycles. Therefore, MIEX resin can be considered as an economical adsorbent for GA removal.

Mechanism of GA adsorption on MIEX resin

In order to explore whether ion exchange dominates the mechanism of GA adsorption on MIEX resin, the amounts of GA adsorbed on MIEX resin and chloride ions releasing into aqueous solution from the surface of resin before and after adsorption are calculated at different GA concentrations. And the results are shown in Figure 8. Figure 8 shows that the amount of GA adsorbed on MIEX resin is approximately equal to the amount of chloride ions entering into the solution at different initial GA concentrations. This

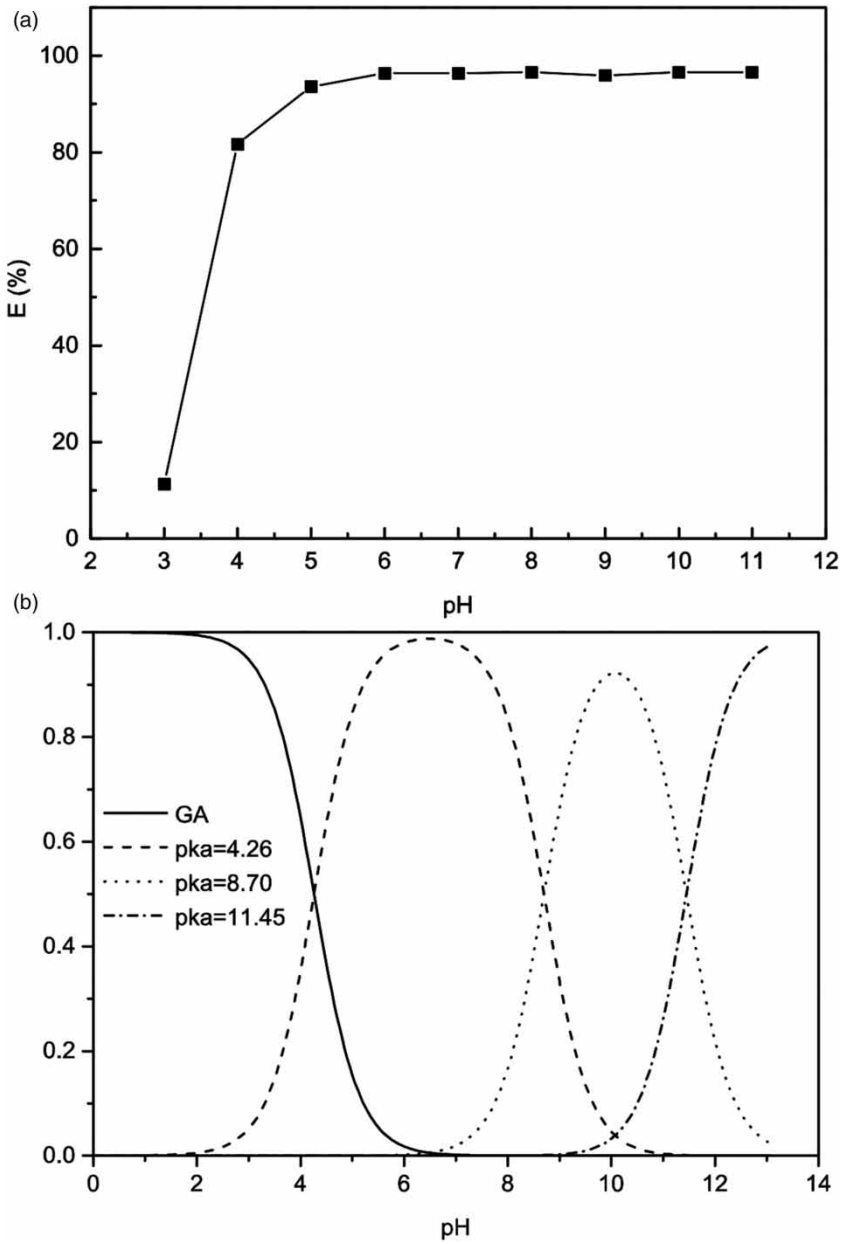

Figure 5 | Effect of pH on (a) GA removal efficiency and (b) theoretical distribution of GA species.

indicates that the ion exchange dominates the removal mechanism of GA.

Comparison with other absorbents

The maximum adsorption capacity and adsorption equilibrium time of GA adsorbed on MIEX resin are compared with other adsorbents in previous literature (Michailof *et al.* 2008; Wang *et al.* 2009; Cagnon *et al.* 2011; Han *et al.* 2017), and the results are shown in Table 6. It can be seen from Table 6 that the MIEX resin has a much higher adsorption capacity (192.19 mg g^{-1}) and much shorter adsorption time (2 h) compared with other absorbents, indicating that MIEX resin is a potential adsorbent for removing GA from water.

CONCLUSIONS

In this study, the adsorptive removal of GA by MIEX resin was investigated, and some conclusions were obtained as

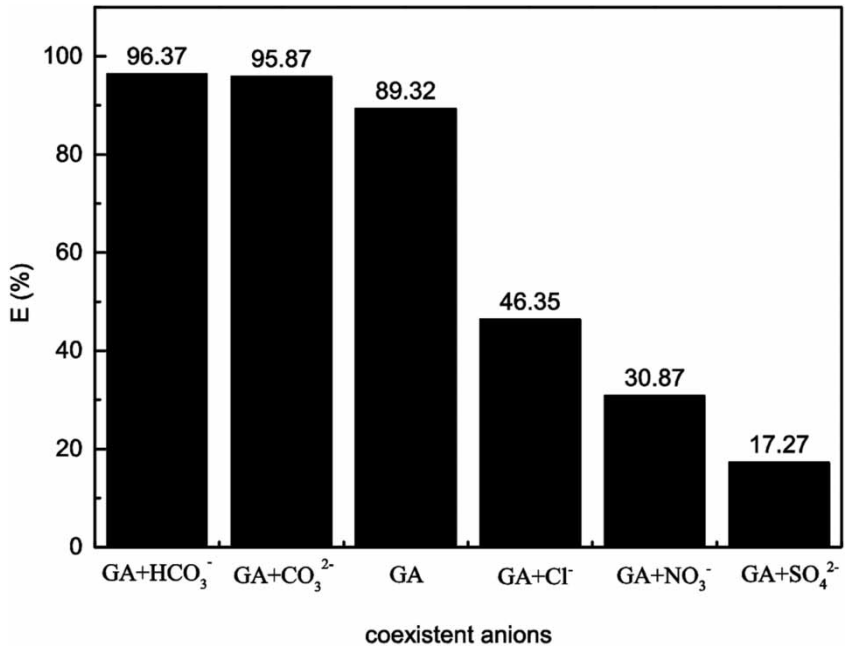

Figure 6 | Effect of inorganic anion on the removal of GA.

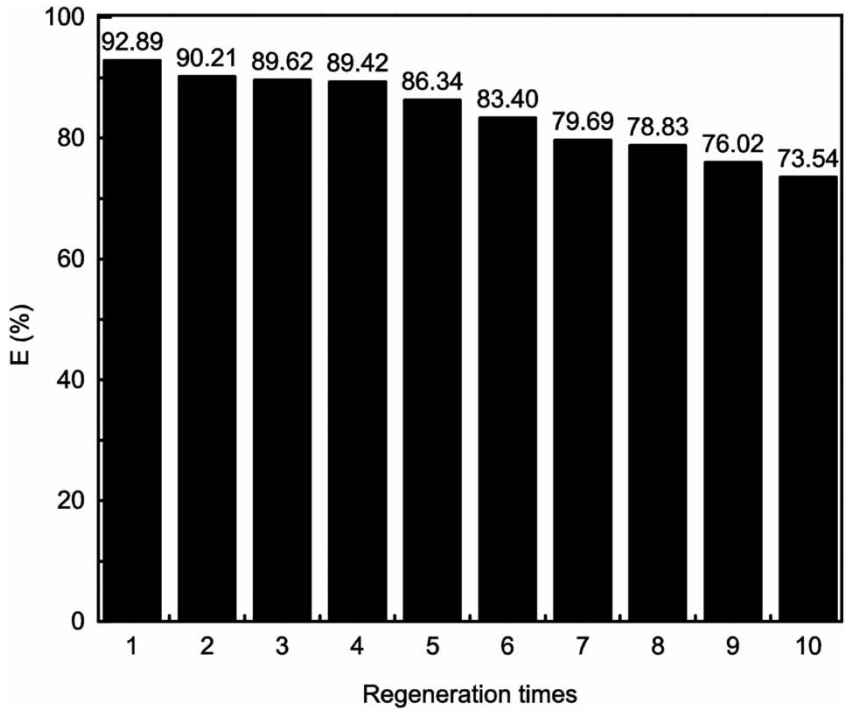

Figure 7 | Effect of regeneration times on the removal of GA by MIEX resin.

follows. The amount of GA adsorbed on MIEX resin increased with increasing the initial GA concentration. Although the different initial GA concentrations had slight effect on the needed time to reach equilibrium, 120 min was sufficient to attain equilibrium. Elevating temperature favored the removal of GA. MIEX resin demonstrated

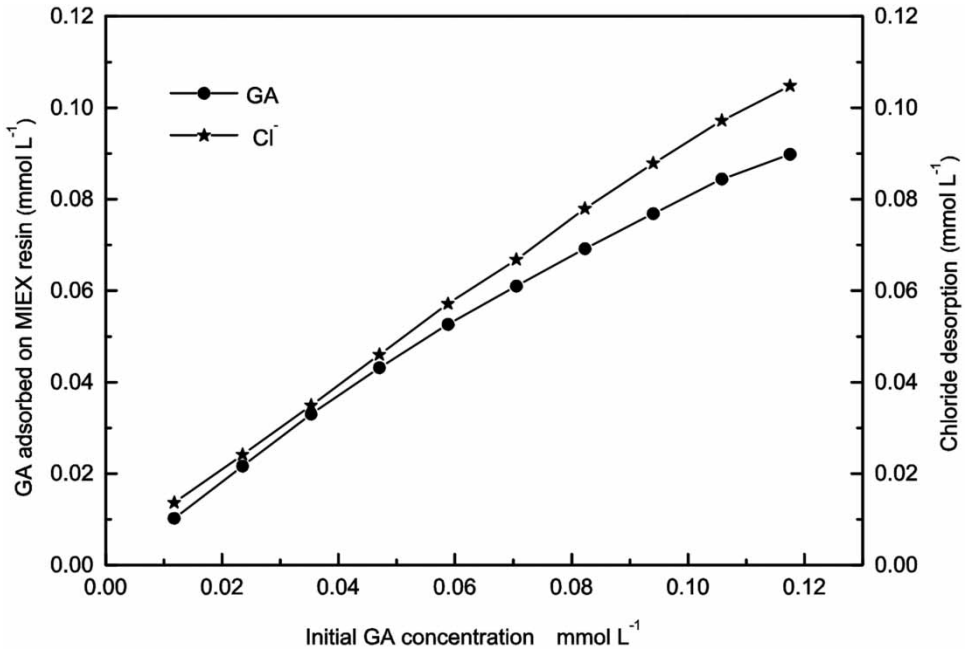

Figure 8 | Quantitative analysis of GA adsorbed on MIEX resin and chloride ions in solution at adsorption equilibrium.

Table 6 | Maximum adsorption capacities (q_{max}) of GA on different adsorbents

Adsorbent	Adsorption time	q_{max} (mg g^{-1})	References
Carbon C9	24 h	109.85	Michailof *et al.* (2008)
WJN-09	120 h	97	Wang *et al.* (2009)
P 150-0	7 h	317.9	Cagnon *et al.* (2011)
P 150-4	7 h	464.1	Cagnon *et al.* (2011)
HF-02	24 h	160.1	Han *et al.* (2017)
MIEX resin	2 h	192.19	This work

high efficiency for the removal of GA at a wide range of pH (5–11). The carbonate and bicarbonate in aqueous solution promoted the removal of GA. However, the chloride, sulfate and nitrate had significant negative effects on the adsorption of GA on MIEX resin. The kinetics process followed the pseudo second-order model, and the film diffusion governed the whole adsorption rate. The equilibrium of GA adsorbed on MIEX resin could be well described by the Redlich–Peterson model. The adsorption was a spontaneous, endothermic and entropy driven process. The ion exchange dominated the removal mechanism. The regenerated MIEX resin could maintain relatively high GA removal efficiency even after 10 adsorption–desorption cycles. In future research, the removal of GA in a continuous operation process for real water needs to be studied.

ACKNOWLEDGEMENTS

This work was supported by the National Natural Science Foundation of China (grant no. 51308001), the project of cultivating top talents for the universities in Anhui Province (grant no. gxyqZD2017036), the Innovation Research Funds of Anhui University of Technology for Graduate (2017052), and the Innovation and Entrepreneurship Training Program of China for Undergraduate (201810360073).

REFERENCES

Abdi, S., Nasiri, M., Mesbahi, A. & Khani, M. H. 2017 Investigation of uranium (VI) adsorption by polypyrrole. *Journal of Hazardous Materials* **332** (June), 132–139.

Ahmat, A. M., Thiebault, T. & Guégan, R. 2019 Phenolic acids interactions with clay minerals: a spotlight on the adsorption mechanisms of gallic acid onto montmorillonite. *Applied Clay Science* **180**, 105188.

Akram, M., Bhatti, H. N., Iqbal, M., Noreen, S. & Sadaf, S. 2017 Biocomposite efficiency for Cr(VI) adsorption: kinetic, equilibrium and thermodynamics studies. *Journal of Environmental Chemical Engineering* **5** (1), 400–411.

Boyer, T. H. 2015 Removal of dissolved organic matter by magnetic ion exchange resin. *Current Pollution Reports* **1** (3), 142–154.

Cagnon, B., Chedeville, O., Cherrier, J.-F., Caqueret, V. & Porte, C. 2011 Evolution of adsorption kinetics and isotherms of gallic acid on an activated carbon oxidized by ozone: comparison

to the raw material. *Journal of the Taiwan Institute of Chemical Engineers* **42** (6), 996–1003.

Celestino, G. G., Henriques, R. R., Shiguihara, A. L., Constantino, V. R. L., de Siqueira Melo, R. & Amim Junior, J. 2018 Adsorption of gallic acid on nanoclay modified with poly(diallyldimethylammonium chloride). *Environmental Science and Pollution Research International* **26** (28), 28444–28454.

Chedri Mammar, A., Mouni, L., Bollinger, J.-C., Belkhiri, L., Bouzaza, A., Assadi, A. A. & Belkacemi, H. 2019 Modeling and optimization of process parameters in elucidating the adsorption mechanism of gallic acid on activated carbon prepared from date stones. *Separation Science and Technology*, doi: 10.1080/01496395.2019.1676785.

Ding, L., Wu, C., Deng, H. & Zhang, X. 2012 Adsorptive characteristics of phosphate from aqueous solutions by MIEX resin. *Journal of Colloid and Interface Science* **376** (1), 224–232.

Ding, L., Zhu, Y., Du, B., Ma, J. & Zhang, X. 2017 Removal characteristics of tanic acid adsorbed on MIEX resin. *Polish Journal of Environmental Studies* **26** (3), 1031–1043.

Doke, K. M. & Khan, E. M. 2017 Equilibrium, kinetic and diffusion mechanism of Cr (VI) adsorption onto activated carbon derived from wood apple shell. *Arabian Journal of Chemistry* **10**, S252–SS60.

El-Shahawi, M. S. & Nassif, H. A. 2003 Retention and thermodynamic characteristics of mercury(II) complexes onto polyurethane foams. *Analytica Chimica Acta* **481** (1), 29–39.

Fazary, A. E. & Ju, Y.-H. 2008 Nonaqueous solution studies on the protonation equilibria of some phenolic acids. *Journal of Solution Chemistry* **37** (9), 1305–1319.

Foo, K. Y. & Hameed, B. H. 2010 Insights into the modeling of adsorption isotherm systems. *Chemical Engineering Journal* **156** (1), 2–10.

Gao, Z. P., Yu, Z. F., Yue, T. L. & Quek, S. Y. 2013 Adsorption isotherm, thermodynamics and kinetics studies of polyphenols separation from kiwifruit juice using adsorbent resin. *Journal of Food Engineering* **116** (1), 195–201.

Gil, A., Taoufik, N., García, A. & Korili, S. 2019 Comparative removal of emerging contaminants from aqueous solution by adsorption on an activated carbon. *Environmental Technology* **40** (23), 3017–3030.

Hamayun, M., Mahmood, T., Naeem, A., Muska, M., Din, S. & Waseem, M. 2014 Equilibrium and kinetics studies of arsenate adsorption by $FePO_4$. *Chemosphere* **99**, 207–215.

Han, F., Xu, C., Sun, W.-Z., Yu, S.-T. & Xian, M. 2017 Effective removal of salicylic and gallic acids from single component and impurity-containing systems using an isatin-modified adsorption resin. *RSC Advances* **7** (37), 23164–23175.

Ignat, I., Neagu, V., Bunia, I., Paduraru, C., Volf, I. & Popa, V. I. 2011 A comparative study on adsorption of gallic acid onto polymeric adsorbents with amine functional groups. *Cellulose Chemistry and Technology* **45** (3), 251.

Kim, S.-H. & Choi, P.-P. 2017 Enhanced Congo red dye removal from aqueous solutions using iron nanoparticles: adsorption, kinetics, and equilibrium studies. *Dalton Transactions* **46** (44), 15470–15479.

Li, L., Liu, S. & Zhu, T. 2010 Application of activated carbon derived from scrap tires for adsorption of Rhodamine B. *Journal of Environmental Sciences* **22** (8), 1273–1280.

Li, X., Liu, Z. & Lee, J. Y. 2013 Adsorption kinetic and equilibrium study for removal of mercuric chloride by $CuCl_2$-impregnated activated carbon sorbent. *Journal of Hazardous Materials* **252–253**, 419–427.

López-Ortiz, C., Sentana-Gadea, I., Varó-Galvañ, P. J., Maestre-Pérez, S. & Prats-Rico, D. 2018 Effect of magnetic ion exchange (MIEX®) on removal of emerging organic contaminants. *Chemosphere* **208**, 433–440.

Michailof, C., Stavropoulos, G. G. & Panayiotou, C. 2008 Enhanced adsorption of phenolic compounds, commonly encountered in olive mill wastewaters, on olive husk derived activated carbons. *Bioresource Technology* **99** (14), 6400–6408.

Perez-Aguilar, N. V., Diaz-Flores, P. E. & Rangel-Mendez, J. R. 2011 The adsorption kinetics of cadmium by three different types of carbon nanotubes. *Journal of Colloid and Interface Science* **364** (2), 279–287.

Prasad, R. K. & Srivastava, S. 2009 Sorption of distillery spent wash onto fly ash: kinetics and mass transfer studies. *Chemical Engineering Journal* **146** (1), 90–97.

Rewatkar, K., Shende, D. Z. & Wasewar, K. L. 2016 Effect of temperature on reactive extraction of gallic acid using tri-n-butyl phosphate, tri-n-octylamine and Aliquat 336. *Journal of Chemical & Engineering Data* **61** (9), 3217–3224.

Riahi, K., Chaabane, S. & Thayer, B. B. 2017 A kinetic modeling study of phosphate adsorption onto *Phoenix dactylifera* L. date palm fibers in batch mode. *Journal of Saudi Chemical Society* **21**, S143–S152.

Senthil Kumar, P., Ramalingam, S., Senthamarai, C., Niranjanaa, M., Vijayalakshmi, P. & Sivanesan, S. 2010 Adsorption of dye from aqueous solution by cashew nut shell: studies on equilibrium isotherm, kinetics and thermodynamics of interactions. *Desalination* **261** (1–2), 52–60.

Shahamirifard, S. A., Ghaedi, M., Razmi, Z. & Hajati, S. 2018 A simple ultrasensitive electrochemical sensor for simultaneous determination of gallic acid and uric acid in human urine and fruit juices based on zirconia-choline chloride-gold nanoparticles-modified carbon paste electrode. *Biosensors and Bioelectronics* **114**, 30–36.

Singh, S. & Kushwaha, J. P. 2014 Tannic acid adsorption/desorption study onto/from commercial activated carbon. *Desalination and Water Treatment* **52** (16–18), 3301–3311.

Sun, C., Zhang, G., Qu, R. & Yu, Y. 2011 Removal of transition metal ions from aqueous solution by crosslinked polystyrene-supported bis-8-oxyquinoline-terminated open-chain crown ethers. *Chemical Engineering Journal* **170** (1), 250–257.

Tan, K. L. & Hameed, B. H. 2017 Insight into the adsorption kinetics models for the removal of contaminants from aqueous solutions. *Journal of the Taiwan Institute of Chemical Engineers* **74**, 25–48.

Tang, Y., Liang, S., Guo, H., You, H., Gao, N. & Yu, S. 2013 Adsorptive characteristics of perchlorate from aqueous

solutions by MIEX resin. *Colloids and Surfaces A: Physicochemical and Engineering Aspects* **417**, 26–31.

Viegas, R. M. C., Campinas, M., Costa, H. & Rosa, M. J. 2014 How do the HSDM and Boyd's model compare for estimating intraparticle diffusion coefficients in adsorption processes. *Adsorption* **20** (5–6), 737–746.

Wang, J., Li, A., Xu, L. & Zhou, Y. 2009 Adsorption of tannic and gallic acids on a new polymeric adsorbent and the effect of Cu(II) on their removal. *Journal of Hazardous Materials* **169** (1–3), 794–800.

Yoro, K. O., Amosa, M. K., Sekoai, P. T., Mulopo, J. & Daramola, M. O. 2020 Diffusion mechanism and effect of mass transfer limitation during the adsorption of CO_2 by polyaspartamide in a packed-bed unit. *International Journal of Sustainable Engineering* **13** (1), 54–67.

Yu, J., Zhang, X., Wang, D. & Li, P. 2018 Adsorption of methyl orange dye onto biochar adsorbent prepared from chicken manure. *Water Science and Technology* **77** (5–6), 1303–1312.

Zhang, Z., Pang, Q., Li, M., Zheng, H., Chen, H. & Chen, K. 2015 Optimization of the condition for adsorption of gallic acid by *Aspergillus oryzae* mycelia using Box-Behnken design. *Environmental Science and Pollution Research* **22** (2), 1085–1094.

Zhang, Y., He, P., Jia, L., Zhang, T., Liu, H., Wang, S., Li, C., Dong, F. & Zhou, S. 2019 Dimensionally stable Ti/SnO_2-RuO_2 composite electrode based highly efficient electrocatalytic degradation of industrial gallic acid effluent. *Chemosphere* **224**, 707–715.

Zhu, Y., Gao, N., Wang, Q. & Wei, X. 2015 Adsorption of perchlorate from aqueous solutions by anion exchange resins: effects of resin properties and solution chemistry. *Colloids and Surfaces A: Physicochemical and Engineering Aspects* **468**, 114–121.

First received 15 October 2019; accepted in revised form 1 May 2020. Available online 15 May 2020